



# Identification of damping elements in a CNC machine tool drive

G. Holroyd, C. Pislaru & D.G. Ford

*Precision Engineering Centre, University of Huddersfield, UK*

## Abstract

An understanding of the dynamic characteristics of a machine tool is a vital element in the control of the machine which has a direct affect on the precision of the machining which can be undertaken. The ways in which energy is dissipated, such as friction and damping, have a significant effect on the dynamic behaviour. This paper outlines an approach to investigating the dynamic characteristics of an axis drive on a CNC milling machine. The torsional behaviour of the motor, belt drive and ballscrew coupled with the axial movement of the table or saddle and the ballscrew nut were considered. The mechanical elements of the drive were modelled as point inertias coupled by springs and dampers using Matlab/Simulink. The undamped natural frequencies and their likely mode shapes were determined using an eigenvalue approach in order to act as a guide to the numbers we were likely to get. The effect of the distributed mass in the ballscrew was also investigated. Comparison with measurements gave values of the dynamic stiffness and damping factor governing the lowest of the observed natural frequencies. The approach outlined in the paper is being used as a basis for investigations into other aspects of the dynamic behaviour of machine tool drives.

## 1 Introduction

The machine tool drives considered in this Paper are the X and Y drives of a Beaver VC35 CNC milling machine in use at Huddersfield University's Precision Engineering Centre.

The Beaver machine is a CNC milling machine which has a vertical spindle mounted on a fixed column, see Figure 1. Vertical (Z direction) motion of the

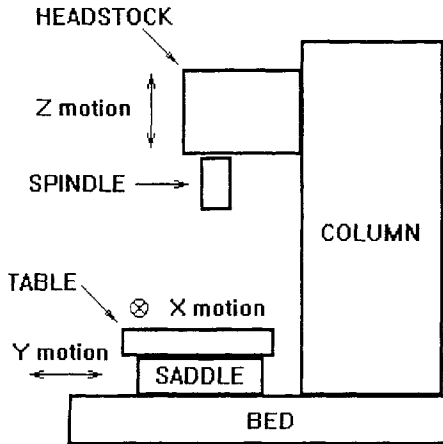


Figure 1: The Beaver VC35 CNC milling machine

cutting head is achieved by moving it up and down a vertical slideway on the front face of the column. Horizontal movement of the workpiece relative to the cutting head is achieved by moving the table from side to side (X direction) and backwards and forwards (Y direction) in front of the column. X motion is given by the table moving on a saddle which in turn rests on the machine bed. Y motion is given by moving the saddle.

The drive for both X and Y direction consists of a DC electric motor which drives a ballscrew via a belt drive, the ballscrew then driving the table (X drive) or saddle (Y drive), see Figure 2.

The aim of this investigation was to quantify the damping elements in a machine tool drive. Two types of damping were considered, Coulomb friction and viscous damping. To gain understanding of the vibration behaviour to be expected, the undamped natural frequencies [1] at which vibration might occur and their associated mode shapes were calculated. The machine drive was then modelled using simulation techniques and the results compared with measured values

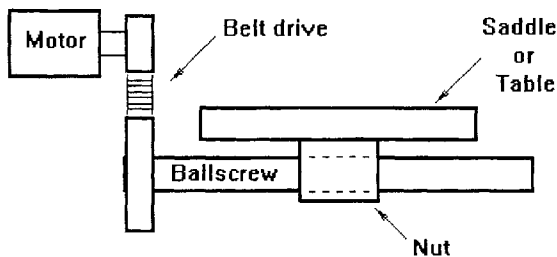


Figure 2: X and Y axis drives

## 2 Coulomb friction

Friction takes place along two mating surfaces where relative movement might occur.

Let the surfaces be held in contact by a normal force  $F_n$ . When a force  $F$  is applied parallel to the surfaces where there is **not** any relative motion, the force  $F_t$  transmitted across the interface is

$$\begin{aligned} F_t &= F, \text{ when } F \leq \mu \times F_n \\ F_t &= \mu F_n, \text{ when } F > \mu \times F_n \end{aligned} \quad (1)$$

where  $\mu$  is the coefficient of friction. When a force  $F$  is applied parallel to the surfaces where there is relative motion, the force  $F_t$  transmitted across the interface is

$$F_t = \mu F_n, \text{ opposed to the direction of motion,} \quad (2)$$

## 3 Viscous damping

Viscous damping gives rise to a force which is proportional to the relative velocity of two parts of a system. It can be introduced deliberately as, for example, in the case of a hydraulic damper or “shock absorber” in a vehicle suspension, or it might occur naturally as the result of the dissipative properties of the component’s material.

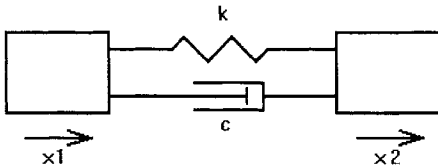


Figure 3: Spring and damper element

In this investigation a viscous damper is considered in parallel with a spring.

The force  $F$  generated by the spring / damper is

$$F = k \times (x_2 - x_1) + c \times \left( \frac{dx_2}{dt} - \frac{dx_1}{dt} \right), \quad (3)$$

where  $x_1$  and  $x_2$  = displacements,  
 $k$  = the spring stiffness,  
 $c$  = the damping coefficient and  
 $t$  = time.



## 4 Identification of the undamped natural frequencies

It is a useful first step to find the frequencies at which vibration might occur, especially for the cases where damping is relatively light. It is also useful to determine the **mode shapes** [2] associated with each natural frequency. These give us an idea of where in the system the greatest vibratory activity may be seen. Both natural frequencies and mode shapes can be calculated using an **eigenvalue method** [3, 4, 5].

### 4.1. Eigenvalue method

First, the system is considered to act as if the inertia is gathered into a set of discrete points - e.g. the motor, the driving pulley, the driven pulley and the ballscrew. Then an equation of motion is written for each point inertia. Grouping them into matrix form gives

$$\mathbf{J} \frac{d^2 \boldsymbol{\theta}}{dt^2} + \mathbf{K}_\theta \boldsymbol{\theta} = \mathbf{f}(t) \quad (4)$$

where

$\mathbf{J}$  is the inertia matrix, a diagonal matrix of the form  $(J_{ii})$ ,

$\mathbf{K}_\theta$  is the stiffness matrix of the form  $(K_{\theta ij})$ ,

$\boldsymbol{\theta}$  is the angular displacement vector and

$\mathbf{f}(t)$  is the forcing term vector.

Solutions are of the form  $\boldsymbol{\theta} = (\phi_i e^{j\omega t})$  when  $\mathbf{f}(t) = \mathbf{0}$ . Substituting into the equation of motion gives rise to

$$(\mathbf{K}_\theta - \mathbf{J}\omega^2)\boldsymbol{\theta} = \mathbf{0} \quad (5)$$

We now divide each equation by the square root of its inertia term  $J_{ii}$  and replace  $\boldsymbol{\theta}$  by  $\boldsymbol{\theta}' = (\sqrt{J_{ii}} \times \phi_i e^{j\omega t})$ . In matrix form the equation now becomes

$$(\mathbf{K}_{\text{mod}} - \mathbf{I}\omega^2)\boldsymbol{\theta}' = \mathbf{0} \quad (6)$$

where

$\mathbf{K}_{\text{mod}}$  is derived from  $\mathbf{K}_\theta$  by dividing its rows and columns by  $\sqrt{J_{ii}}$  and  $\mathbf{I}$  is the unity matrix. This is an eigenvalue equation.

### 4.2. Solution of eigenvalue equation

The eigenvalue equation has a non-trivial solution for  $\mathbf{x}$  when

$$\left| (\mathbf{K}_{\text{mod}} - \mathbf{I}\omega^2) \right| = 0 \quad (7)$$

In this case  $\mathbf{K}_{\text{mod}}$  is real and symmetric and there are standard “black box” solutions to such equations available in many mathematics software packages. The number of solutions for  $\omega^2$  is equal to the order of matrix  $\mathbf{K}_{\text{mod}}$  although not all of them are bound to be distinct. To each value of  $\omega^2$  there is a vector which gives the mode shape of  $\theta'$  for that frequency. The mode shape in terms of angle  $\theta$  is obtained by dividing each term in  $\theta'$  by  $\sqrt{J_{ij}}$ .

### 4.3 Torsional analysis of X drive

There are five main inertia elements in the drive: the motor, the driving pulley, driven pulley, the ballscrew and the ballscrew load, (i.e. the table referred to the ballscrew rotation by multiplying the linear inertia by  $(\text{pitch}/(2\pi))^2$ ). There are three main stiffness elements: the motor shaft, the belt drive and the ballscrew.

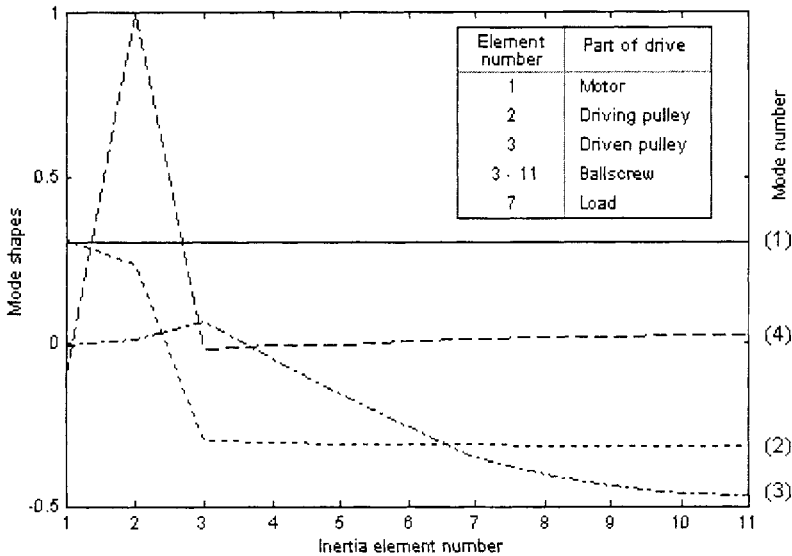


Figure 4: Results of undamped natural frequency analysis

The model set up had the motor, pulleys and load represented as single lumped inertias and the ballscrew divided into 9 pieces with the ballscrew flexibility apportioned between each. The load was set in a central position along the length of the ballscrew

The first four natural frequencies (see Figure 4) are

1. (solid line) 0 Hz “roll” mode
2. (dotted line) 79 Hz motor and driving pulley v. driven pulley and ballscrew
3. (chain line) 439 Hz ballscrew twist
4. (broken line) 582 Hz driving pulley “bounce”

## 5 Modelling the machine drive using simulation techniques

### 5.1 Inertia elements

The inertia elements are represented by a modelling block such as

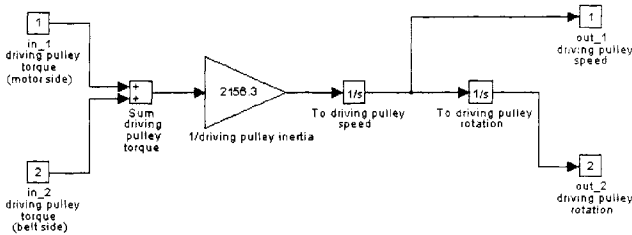


Figure 5: Simulink modelling sub-system – inertia element

### 5.2 Spring / damper elements

The spring /damper elements are represented by a modelling block such as

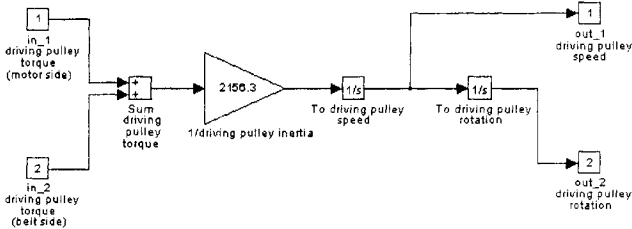


Figure 6: Simulink modelling sub-system – spring / damper element

### 5.3 Coulomb friction elements

A Coulomb friction element can be represented by a modelling block such as

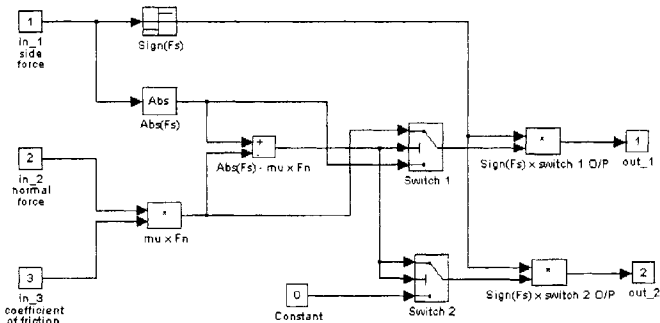


Figure 7: Simulink modelling sub-system – spring / damper element

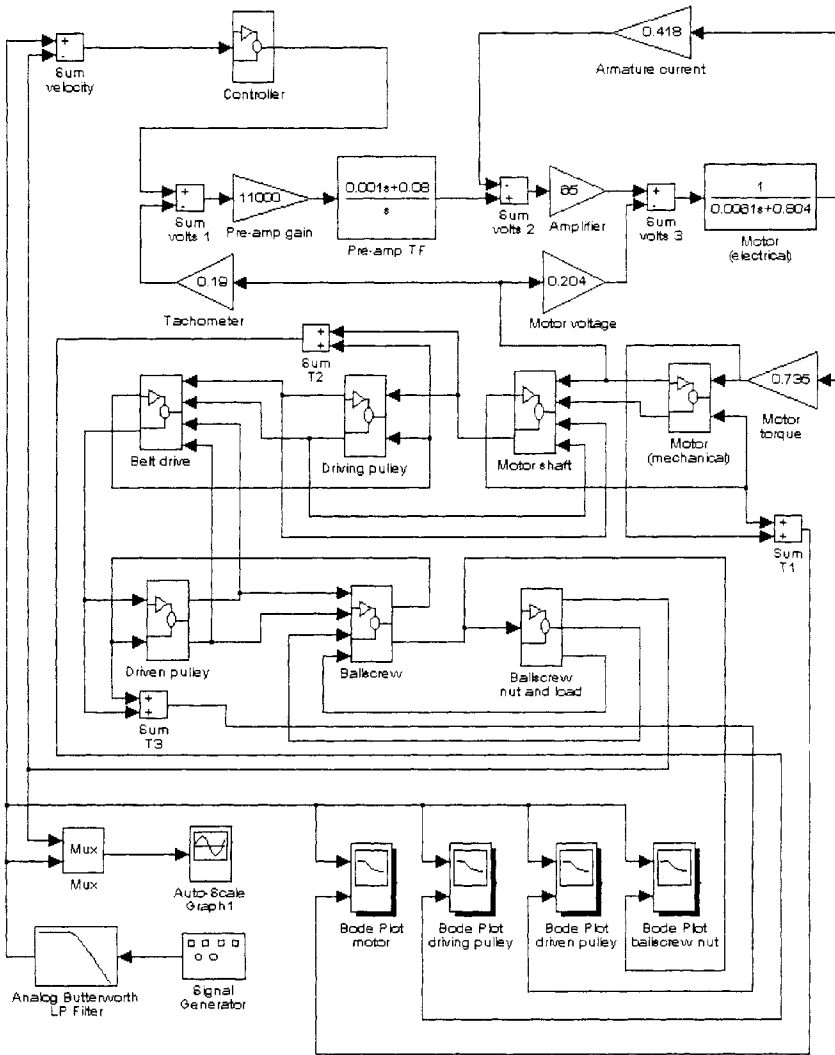


Figure 8: A typical model, this one looking at torsional vibration

## 6 Measurements

Torsional excitation has been applied to the motor by injecting a swept sine signal from a Transfer Function Analyser into the machine drive. Measurements of the vibration were made using accelerometers attached to the pulleys on the motor shaft and the ballscrew. These were set in a circumferential direction so that torsional and radial movement could be monitored, (see Figure 9).

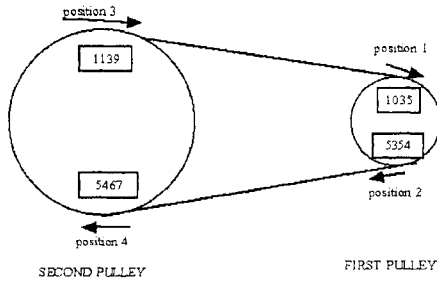


Figure 9: Arrangement of accelerometers

## 7 Results

The experimental results came in the form of Bode plots.

It was possible to produce Bode plots from the models by two ways. First by linearising the model using a special Matlab routine and using Matlab's Bode routine to print the result. The second was to apply an excitation to the Simulink model and take a Bode plot of the results using Simulink 1's Bode feature.

By comparing the acceleration picked up by the two accelerometers on the driving pulley, we were able to show that the vibration was principally torsional, (see Figure 10). (The dip in the transfer functions in Figures 10 and 11 at the low frequency end is due to electrical effects in the vibration measuring systems and is not a mechanical effect.)

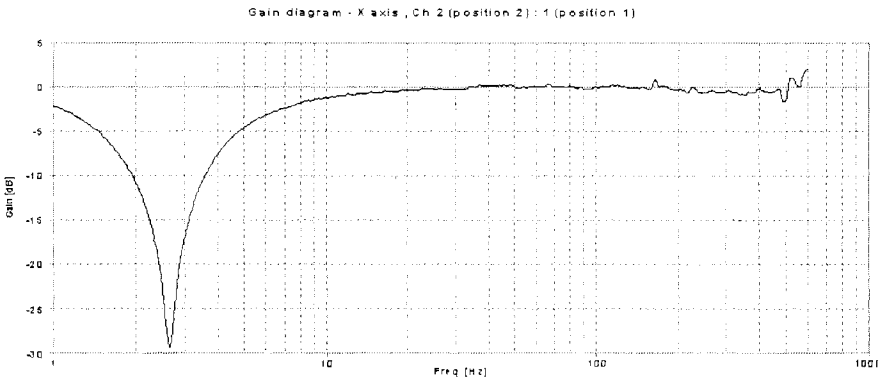


Figure 10: Transfer function between two circumferentially set accelerometers on the motor shaft pulley

By comparing the acceleration picked up by one of the accelerometers on the driving (first) pulley with that from one on the driven (second) pulley we were able to observe the vibration characteristics of the drive belt, (see Figure 11).

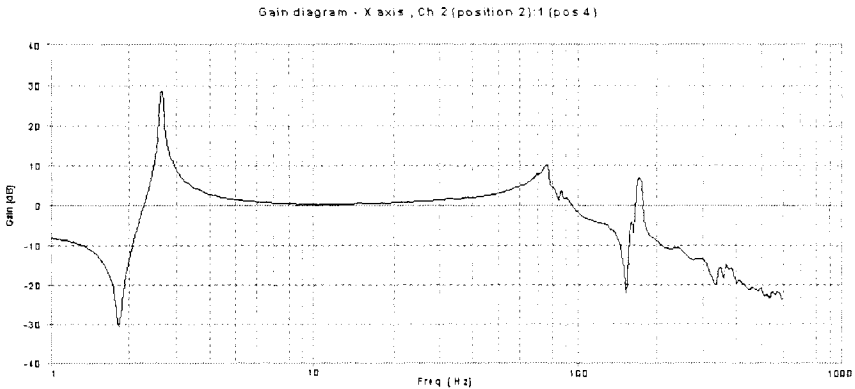


Figure 11: Transfer function between circumferentially set accelerometers on the motor shaft and ballscrew pulleys

## 8 Discussion of results

A peak in the belt drive transfer function was observed at 79 Hz for the X drive. Starting with this result it was possible to use Matlab to refine an initially too low estimate of the belt stiffness. With the revised stiffness included in a Simulink model it was possible to estimate a value of 0.16 for the damping factor  $\zeta$  of the belt drive. The behaviour of the belt was more complicated than suggested by the theory used to derive its effective torsional stiffness. Transverse vibration of the belt may be responsible for some of the other vibration peaks observed in the measurements. The possibility of the belt's going slack on one side then the other as it vibrates may bring in non-linear behaviour.

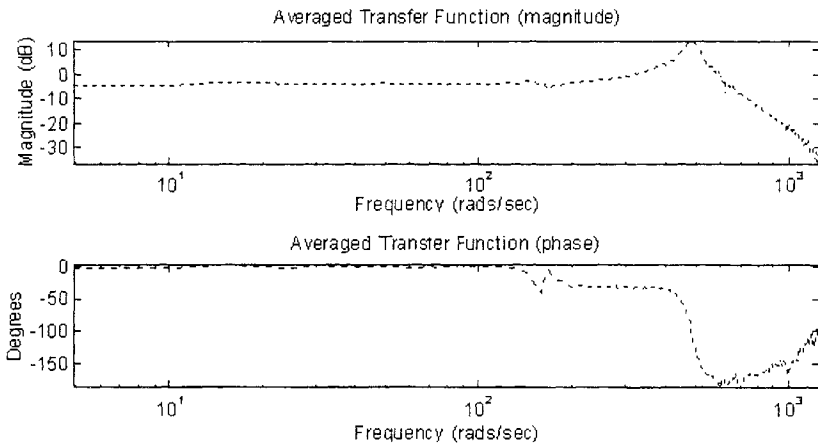


Figure 12: Transfer function between ballscrew and motor shaft predicted by a Simulink model

298 *Laser Metrology and Machine Performance*

A Simulink model which included the Coulomb friction to be expected between the table and saddle (X drive) or the saddle and table (Y drive) showed that, at low levels of movement at least, friction tended to generate vibration as well as dissipating vibratory energy. This arose because potential energy is built up in the flexible parts of the system until enough force is generated to overcome friction. In addition, kinetic energy is built up as the ballscrew moves through its backlash.

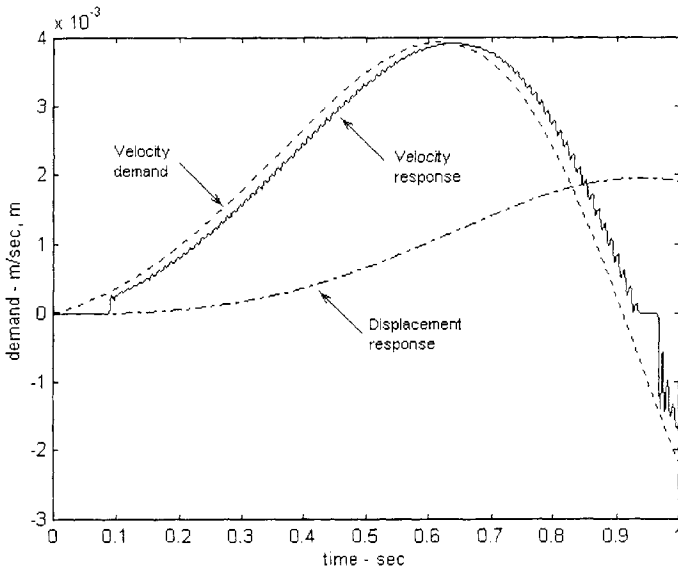


Figure 13: First second of table movement for X drive under swept sine excitation

A perturbation signal of about 250 mV was injected at the preamplifier. (This was the most that could be applied in closed loop without tripping the controller.) One of the Simulink models was set to give the amount of angular movement observed to be caused by the injected signal at the driving pulley. Figure 13 shows the movement of the table predicted by the same model under these conditions. The controller step time is 10 msec. A further 80 msec delay occurs before the table starts with a jerk. The velocity response is damped down quickly after the initial step, but continues to exhibit vibratory behaviour on top of a typical time delayed response.

The same model also predicted that the table or saddle would cease to vibrate above a certain frequency under swept sine excitation due to the backlash in the ballscrew nut. This was observed to happen when measurements were taken.

Refinements of the model which calculated the energy balance in the motion showed that, with the correct choice of solver, an energy balance was maintained. The models proved to be mathematically robust in the sense that they could handle a step demand to full table speed without exhibiting numerical instability.

The Advanced Manufacturing Technology Research Institute (AMTRI) has done a modal analysis of the machine [6]. They have identified several natural frequencies with their mode shapes and associated damping.

However, these modes mainly involved "whole body" movement of parts of the machine. In general these modes could involve bending or twisting of the saddle or table, but it was considered that these modes would only have an effect on transverse vibration which was found to be low in the tests covered here.

## 9 Conclusions

- The principal natural frequency and its damping factor were measured for the Beaver machine X and Y drives.
- Transverse vibration levels were low
- A set of well-behaved models was produced which modelled the main vibration characteristics of the system.
- Friction can act as a vibration stimulant as well as being an energy absorbing mechanism.
- Backlash can also act as a vibration stimulant.
- Several building blocks were prepared for use with more sophisticated models in the future, e.g. transverse inertia and spring elements, a non-linear belt element and a hydraulic drag element.
- A more comprehensive model of the drive belt is needed taking into account the belt tension and friction between the belt and pulley, as well as the viscous effect used by the models reported in this paper.

The results of this investigation are being fed into a larger project in hand at Huddersfield University which to improve our understanding of the mechanisms involved in dynamic errors in machine tools.

## 10 References

- [1], [2] Harris C. M., "Shock and vibration handbook", 3<sup>rd</sup> edition, McGraw-Hill, pp 1-22, 1988
- [3] Quayle J. P. ed, "Kempe's engineers' year book , 1984", 89th edition, Morgan Grampian, pp A2/37-8, 1984
- [4] James M. L., Smith G. M., Wolford J. C., Whaley P. W., "Vibration of mechanical and structural systems: with microcomputer applications", Harper & Row, pp 342 et seq, 1989
- [5] Newland D. E., "Mechanical vibration analysis and computation", Longman Scientific and Technical, pp 99 et seq, 1989
- [6] AMTRI report 4PT 6159, "Modal analysis & frequency response measurements of a Beaver milling machine Type: VC35", February 1999